文章编号：1001－9014(2019)02－0133－06

DOI:10.11972/j.issn.1001－9014.2019.02.001

Approach of beam power combining at short millimeter waves

WANG Long*, DOU Wen-Bin*, MENG Hong-Fu*, GUO Huan

(State Key Laboratory of Millimeter Waves, Southeast University, Nanjing 210096, China)

Abstract: In this paper, an approach of beam power combining based on quasi-optical technology is proposed. It has advantages of low loss, high combining efficiency and relatively easy manufacturing. The analysis, simulation and experimental results are presented at short millimeter waves. High combining efficiency has been obtained.

Key words: short millimeter waves, THz, beam power combining, quasi-optical technique

PACS: 41.20.Jb, 42.25.Ja, 42.79.Dj, 84.40.-X

短毫米波波束功率合成方法

王 龙*, 窦文斌*, 孟洪福*, 郭 欢

(东南大学 毫米波国家重点实验室, 江苏 南京 210096)

摘要:提出了一种基于准光技术的波束功率合成方法.它具有损耗低,合成效率高,相对容易制造等优点.在短毫米波给出了分析、仿真和实验结果,结果表明该方法合成效率高.

关 键 词:短毫米波;太赫兹;波束功率合成;准光技术

中图分类号:TN2, TN92　　**文献标识码**:A

Introduction

In recent years, THz science and technology have made great progress, receiving more attention over the world, for example, THz communication, THz measurements and 3D-printing[1-3]. However, the development of terahertz technology now is limited to the terahertz radiation source for its very small output power. To increase the output power of THz source is still a challenge, thus power combining techniques used in microwave bands are considered. At present, the commonly used power combining technology has three ways as: circuit combining, spatial power combining in a waveguide and quasi-optical power combining.

Power combining technology, based on planar transmission line circuit[4-5], has the advantage of a simple design and processing, while the combining efficiency will drop sharply with the increase of the number-combining stages because of the loss of transmission line in short millimeter wave bands region, and the power divider/combiner network becomes smaller and complexity, difficult to make at short millimeter wave bands. The same difficulty exists for the spatial power combining in a waveguide.

The method of spatial power combining usually works in the way that several numbers of power sources through the amplifier array, with the same amplitude and phase characteristics, radiate to the free space to form a plane wave, and then the space electromagnetic wave energy can be collected by an antenna to achieve power combining[6-10]. In short millimeter wave or THz bands, the array components are very difficult to manufacture due to the fact that the wavelength is already smaller than the typical power device size.

Quasi-optical power combining use a quasi-optical technology to achieve the power distribution and combining[11-15]. A typical technical scheme is to use a periodic phase grating, made from a dielectric sheet, to transform the electromagnetic waves by multiple equal-amplitude in-phase excitation sources into a quasi-plane wave, then converted into the Gaussian beam by a shaped reflective surface. Without the ohmic loss, quasi-optical power combining has the low-loss characteristic. In addition, it has no limit to the distance between radiating elements because the periodic phase grating can make the array beam propagate in the main lobe direction. However, the difficulty of this technique is to achieve efficient beam transformation from a quasi-plane wave to the Gaussian beam in engineering applications and the

Received date: 2018-04-12, **revised date**: 2018-12-20　　**收稿日期**:2018-04-12, **修回日期**:2018-12-20

Foundation items: Supported by National Natural Science Foundation of China (61171025)

Biography: WANG Long (1988-), male, Anhui, China, Ph. D. student. Research area involves Quasi-optical technology and antennas. E-mail: wangl0307@qq.com

* **Corresponding author**: E-mail: wangl0307@qq.com, njdouwb@163.com, menghongfu@163.com

existing transformation efficiency is still not high in short millimeter wave bands or THz bands.

Different from aforementioned quasi-optical power combining technique, a new kind of power combining technology at short millimeter wave is proposed, which combines the power of n beams into one beam, and number n of beams is not limited to the even number. The advantage of the technique is that there is no need to design complex beam transformations and have high combining efficiency compared to other power combining techniques. In this paper, combining principle, in which n beams are combined into one beam, is described, High combining efficiency is demonstrated, and then several kinds of beams power combining structures are proposed and classified. Finally, experiments were done to demonstrate theoretical analysis.

1 Principle

The two orthogonal polarized beams with the same amplitude and phase-distribution, arranged in a certain way in space, propagate through the respective ellipsoid mirror to the same quasi-optical beam grating splitter[16]. The two beams are assumed being coherent and combined at the position of their waist. The one incident beam, which has a polarization perpendicular to the direction of the wire in the grating splitter, is almost completely transmitted, while another incident beam, whose polarization is parallel to the direction of the wire in the grating splitter, is almost reflected. A new combined linearly polarized wave is formed after passing through the grating splitter and its polarization is the vectorial sum of the polarization vector of the transmitted beam and the polarization vector of the reflected beam. The combined beam can be received by a horn, after being converged by an ellipsoid, or be used to participate in the n beams power combining. It is called 2 to1 or 1 + 1 type beam combining.

Take 2 to1 beams combining as an example, the implementation of the schematic is shown in Fig. 1. H1 and H2 represent the wave source horns, launching coherent in-phase orthogonal polarized beam. H3 represents the receiver horn. M1, M2, M3 are ellipsoids mirrors. G1 is a quasi-optical grating splitter. The incident beams from H1 and H2 pass through M1 and M2 to G1, respectively, coaxially at the center of G1, one beam pass through the grating and one beam is reflected by the grating along the same direction, then a combined beam is obtained. The combined beam can be received by the H3 through M3 converged reflection.

It is clear that a Gaussian beam can be applied the same transformation by a mirror or a lens, according to the Gaussian beam theory[17]. Here we use PEC (perfect electric conductor) ellipsoid mirror so that dielectric loss and conductor loss all not exist in our analysis. G1 is placed at the location where the waist of the two transformed Gaussian beam is coincident. In order to express them simply, a local coordinate system u-v-w (w is perpendicular to the paper surface) can be built at the center of G1. Beam B_1 from horn H1 pass through the grating splitter for its polarization is perpendicular to the direction of wire of the grating splitter and propagates along

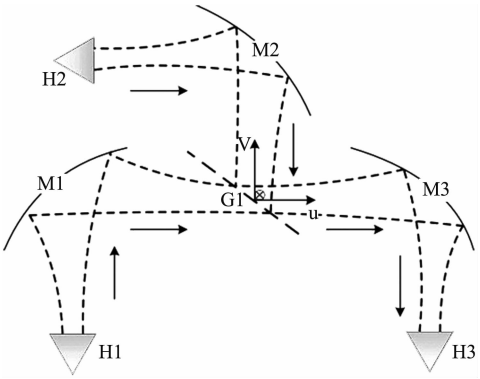

Fig. 1 The schematic diagram of 2 to 1
图1 2合1原理示意图

u direction. The E-field of beam B_1 can be expressed as

$$\vec{\psi}_1 = \hat{v}\frac{\omega_0}{\omega_{u1}}A\exp\left\{-j\left[\frac{\pi r^2}{\lambda R_{u1}} - \arctan\frac{\lambda u_1}{\pi\omega_0^2}\right]\right\} \exp\left[-\frac{r^2}{\omega_{u1}^2}\right]\exp[-jku_1] \quad , \quad (1)$$

where $r = (v^2 + w^2)^{1/2}$, A is the amplitude, ω_0 is the beam waist, R_{u1} is the curvature radius at the u_1 position of u axial and ω_{u1} is the beam radius. Meanwhile, another incident beam B_2 from horn H2 is reflected by the grating splitter for its polarization is parallel to the direction of wire of the grating splitter, it also propagates along u direction, and the E-field of B_2 can be expressed in Eq. 2.

$$\vec{\psi}_2 = \hat{w}\frac{\omega_0}{\omega_{u1}}A\exp\left\{-j\left[\frac{\pi r^2}{\lambda R_{u1}} - \arctan\frac{\lambda u_1}{\pi\omega_0^2}\right]\right\} \exp\left[-\frac{r^2}{\omega_{u1}^2}\right]\exp[-jku_1] \quad , \quad (2)$$

$\hat{w}$ and $\hat{v}$ are unit vectors. It has been assumed in Eqs. 1-2 that the fields of B_1 and B_2 has the same amplitude A and beam parameters such as waist and phase-front. Therefore, the two beams can be combined into a linearly polarized wave beam in the form of Eq. 3

$$\begin{aligned}\vec{E}_{tot} &= \vec{\psi}_1 + \vec{\psi}_2 = (\hat{v} + \hat{w})\frac{\omega_0}{\omega_{u1}}A \\ &\exp\left\{-j\left[\frac{\pi r^2}{\lambda R_{u1}} - \arctan\frac{\lambda u_1}{\pi\omega_0^2}\right]\right\}\exp\left[-\frac{r^2}{\omega_{u1}^2}\right]\exp[-jku_1] \\ &= \frac{1}{\sqrt{2}}(\hat{v} + \hat{w})\left(\sqrt{2}A\frac{\omega_0}{\omega_{u1}}\exp\left[-\frac{r^2}{\omega_{u1}^2}\right]\right) \\ &\exp\left\{-j\left[\frac{\pi r^2}{\lambda R_{u1}} - \arctan\frac{\lambda u_1}{\pi\omega_0^2}\right]\right\}\exp[-jku_1] \\ &= \frac{1}{\sqrt{2}}\vec{T}\left(\sqrt{2}A\frac{\omega_0}{\omega_{u1}}\exp\left[-\frac{r^2}{\omega_{u1}^2}\right]\right) \\ &\exp\left\{-j\left[\frac{\pi r^2}{\lambda R_{u1}} - \arctan\frac{\lambda u_1}{\pi\omega_0^2}\right]\right\}\exp[-jku_1] \quad . \quad (3)\end{aligned}$$

If the amplitude of B_1 and B_2 is different, analysis can be done similarly. For the general situation in practical use, for example, magic-T is added or the transmission path length has a slight change, which can cause

beam B_1 and B_2 have different amplitude (A_1 and A_2) and phase difference of $\Delta\varphi$. Then Eq. 3-1 needs to rewritten by Eq. 4.

$$\begin{aligned}\vec{E}_{\text{tot}} &= \vec{\psi}_1 + \vec{\psi}_2 \\ &= \hat{v}\frac{\omega_0}{\omega_{u1}}A\exp\left\{-j\left[\frac{\pi r^2}{\lambda R_{u1}} - \arctan\frac{\lambda u_1}{\pi\omega_0^2}\right]\right\} \\ &\quad \exp\left[-\frac{r^2}{\omega_{u1}^2}\right]\exp[-jku_1] + \hat{w}\frac{\omega_0}{\omega_{u1}}A_2 \\ &\quad \exp\left\{-j\left[\frac{\pi r^2}{\lambda R_{u1}} - \arctan\frac{\lambda u_1}{\pi\omega_0^2} + \Delta\varphi\right]\right\} \\ &\quad \exp\left[-\frac{r^2}{\omega_{u1}^2}\right]\exp[-jku_1] \\ &= (\hat{v}A_1 + \hat{w}A_2 e^{-j\Delta\varphi})\left(\frac{\omega_0}{\omega_{u1}}\exp\left[-\frac{r^2}{\omega_{u1}^2}\right]\right) \\ &\quad \exp\left\{-j\left[\frac{\pi r^2}{\lambda R_{u1}} - \arctan\frac{\lambda u_1}{\pi\omega_0^2}\right]\right\}\exp[-jku_1] \quad . (4)\end{aligned}$$

Equation 4 indicates that the combined field is elliptically polarized, which can cause some polarization loss by a linearly received horn or be combined in the next step. Thence, some necessary measures may be considered to reduce the phase difference for obtaining high linear polarization during the combining process. Firstly, the phase characteristics of each channel should be measured individually, and then some metal shim can be added at the input port to adjust the phase difference. Thence in the following analysis the same phase of different beams to be combined are assumed.

Vectorial sum of two beams is shown in Fig. 2 (a), if the two beams have a different amplitude, the vectorial sum is denoted in Fig. 2 (b).

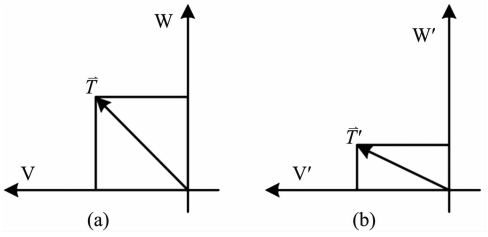

Fig. 2 The combined field vectorial diagram of 2 to 1
图 2 2 合 1 合成场矢量图

Here we assume $\vec{T} = \hat{v} + \hat{w}$, $A_u = A\omega_0/\omega_{u1}$, then the norm of $\vec{T}$ equals $\sqrt{2}$, shown in Fig. 2 (a). The beam energy can be indicated with its E-field multiplied by its conjugated field. Therefore, the power P_1 in B_1 on the coordinate axis is $P_1 = A_u^2$ and the power P_2 in B_2 is $P_2 = A_u^2$. The power P_c in the combined beam can be expressed in Eq. 4.

$$P_c = |\vec{T}|^2 A_u^2 = 2A_u^2 = P_1 + P_2 \quad . \quad (5)$$

Equation 5 demonstrates the law of power conservation. The combined beam can be refocused into the receiving plane by another ellipsoid reflector.

When n beams need to be combined, n is not limited to an even number like conventional power combining method, n can be an odd number or even number according to the requirement to the source power. The structure of n beams combining into one beam is described. The analysis is similar to (1) to (3) above, beam B_1 and beam B_2 have the same beam parameters except for the amplitude. That is, it is just the power combining of two beams with different amplitude. So, we can do 3 beams power combing, 4 beams power combing, 5 beams power combing and till n beams, where n can be a very larger integer number. The every 2 to 1 beam combining happens in each splitter and an independent local coordinate system can be established at each splitter. Two beams to be combined have the same waist size and space position, it can be realized by mirrors or lens. The location of every splitter is uniquely determined by the waist-position of the two incident beams to be combined. For the local coordinate the beam also can be expressed as shown in Eqs. 1-2, the amplitude of two beams can be the same or not. It is same as the forementioned structure that one beam passes through the grating splitter and another beam is reflected by the grating splitter, and the two beams, which have same beam parameters, propagate alone the same direction and form a new combined beam. It is noted that the two beams can have different amplitudes, and the field of the combined beam is the vectorial sum of the two beam field, as stated in Eq. 3.

For example, for 2 + 1 type combining, the beam B_1 is a combined beam as mentioned above, it has amplitude $\sqrt{2}$ and the beam B_2 has amplitude 1, then the field of the combined beam satisfies the Eq. 6, shown in Fig. 2(b).

$$\begin{aligned}\vec{T}' &= \sqrt{2}\hat{v}' + \hat{w}' \Rightarrow |\vec{T}'| = \sqrt{3} \\ P_c &= |\vec{T}'|^2 A_u^2 = 3A_u^2\end{aligned} \quad . \quad (6)$$

Similarly, for $n + m$ type combining,

$$\begin{aligned}\vec{T}' &= \sqrt{n}\hat{v}' + \sqrt{m}\hat{w}' \Rightarrow |\vec{T}'| = \sqrt{n+m} \\ P_c &= |\vec{T}'|^2 A_u^2 = (n+m)A_u^2\end{aligned} \quad . \quad (7)$$

No matter how many beams to be combined, the beams combing is no loss for PEC mirror in theory and low loss for conductor mirror.

2 Simulation

For doing the test conveniently, the simulation is performed at W-band, but not limited to it. The previous analysis shows that a high combining efficiency could be obtained on condition that the grating splitter is fine enough.

The simulation of the above beams' power combining described in Eqs. 3-5 is carried out in the electromagnetic simulation software, Computer Simulation Technology (CST). The radiation horn is designed of reference[18] and the ellipsoidal mirror is designed of reference[19], and the corresponding simulation results are given in Fig. 3. Figure 3(a) shows the radiation pattern of the feed horn, which indicates the circular symmetry, low sidelobe level, and low cross-polarization level. The coupling efficiency between the aperture field of feed horn and Gaussian beam can reach nearly 98%, which is equivalent to Corrugated Horn. Figure 3(b) shows the

characteristics of the grating splitter. The return loss of reflected beam and the transmission loss of transmission beam are both less than −0.15 dB. The phase difference between them is in a straight line, which almost equals 180 degree, in the entire simulation frequency band. The ellipsoidal mirror is used to implement identical transformation for incident Gaussian beam, thence the interception section of the ellipsoid is centered on the minor axis of the ellipsoid. When the aperture diameter is four times beams radius, the efficiency for power transmission can exceed 99%. The left picture in Fig. 3(c) shows the beam transmission reflected by an ellipsoidal mirror and the simulated transmission loss is less than 1 dB in most frequency band from 90 GHz to 100 GHz, while the corresponding test result is shown in another picture and its S_{21} parameter is given.

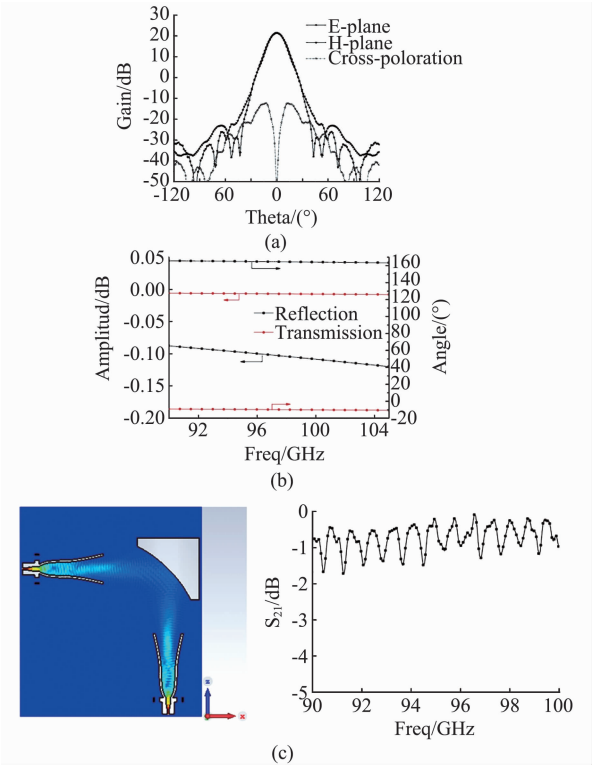

Fig. 3 Results of (a) the simulation of feed horn radiation, (b) the simulation of grating splitter, (c) the simulation and test of ellipsoidal mirror

图3 (a)馈电喇叭辐射仿真,(b)线栅仿真,(c)椭球镜的仿真与测试

The beam combining simulation results are shown in Fig. 4. The quasi-optical grating splitter is placed at the location where the waist of the two transformed Gaussian beam is coincident. Figure 4 (a) shows the whole propagation process in detail from the transmitters to the receiver. Beam_1 and Beam_2 represent the incident beam radiated from the horn 1 and horn 2, respectively. Beam_1 + 2 represents the combined beam after the grating splitter. Moreover, Fig. 4 (b) shows the polarization characteristic of the combined beam in a plane of the receiver. The center distortion is small, and the purity of linear polarization is high. The combining efficiency reflected in the central spot is about 97%.

Then a linearly polarized (45 degree off-axis y) horn antenna, with the same curve as the other radiation horns, is placed below the combined beam and corresponding simulation results are shown in Fig. 5. Figure 5 (a) shows the field distribution in space and (b) shows the S-parameters between the ports. The S_{13} and S_{23} are both among −4.5 dB and −3.2 dB at most frequency bands and they do not achieve its respective maximum at the same time at the center frequency (95 GHz), due to the phase difference caused by the tilted grating splitter. From these results, the system loss for beam combining can be calculated easily, which is less than 1 dB at most frequency bands and the minimum is close to 0.5 dB.

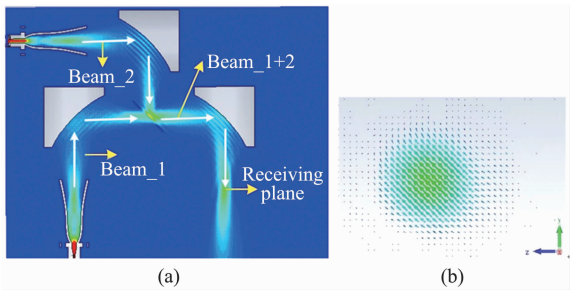

Fig. 4 Simulations results of (a) the beam propagation, and (b) the polarization characteristic

图4 仿真结果(a)波束传播过程,(b)极化特性

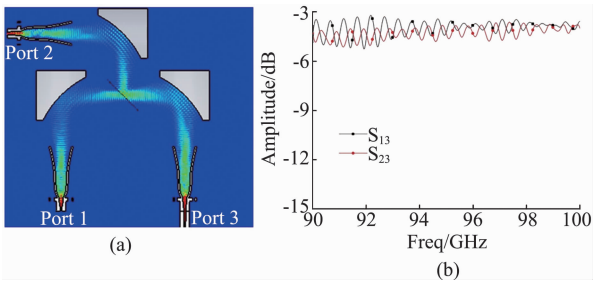

Fig. 5 Simulations results of (a) the field distribution and (b) the S-parameter

图5 仿真结果(a)场分布,(b)S参数

Seen from the simulation results of 2 to 1 beam combining, the scheme is feasible. In order to achieve n beams combining, structural expansion needs to be carried out on this basis. Two categories of structural expansion are considered: one is called $N+1$ ($N \geqslant 1$) beams combining, which is characterized by increasing another way on the basis of the previous way step by step, to form a chain structure in the space; the second category is called $2+N$ type ($N \geqslant 1$) beams combining which is characterized by folding a 2 beams combining to add a N beams combining structure, while the N beams combining structure can be the first category or a second category. Some demonstration configuration in 3D are shown in Fig. 6.

Figure 6 shows the basic composition of the first category. We can easily get Fig. 6(b) from Fig. 4 (a), just by adding one beam. By a cascade connection step by step, N beams combining system can be obtained

when N is big number. Through these simple basic structures, it's possible to bring about more complex and advanced combining system.

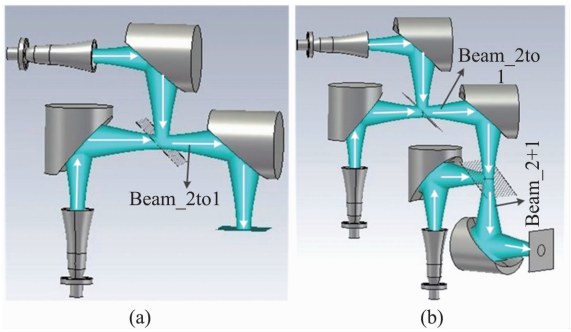

Fig. 6　$N+1$ type (a) 1 +1type, (b) 2 +1 type
图 6　$N+1$ 型(a)1 +1 型,(b)2 +1 型

3 Experiment

The transmission experiment of beam combining is done at W-band, to verify the feasibility of the aforementioned idea of beam power combining and the experimental setup is shown in Fig. 7. The vector network analyzer has been calibrated, and its output signal is divided into two signals by a magic-T. One way is to align the transmission channel where the beam passes through the grating splitter in the quasi-optical device and another way is to align the reflection channel where the beam is reflected by the grating splitter. Because of the position requirement in space, the reflection channel needs to be connected with a long connecting waveguide. One channel is cut off and then the other channel can be tested when the transmission experiment of each single channel is done respectively.

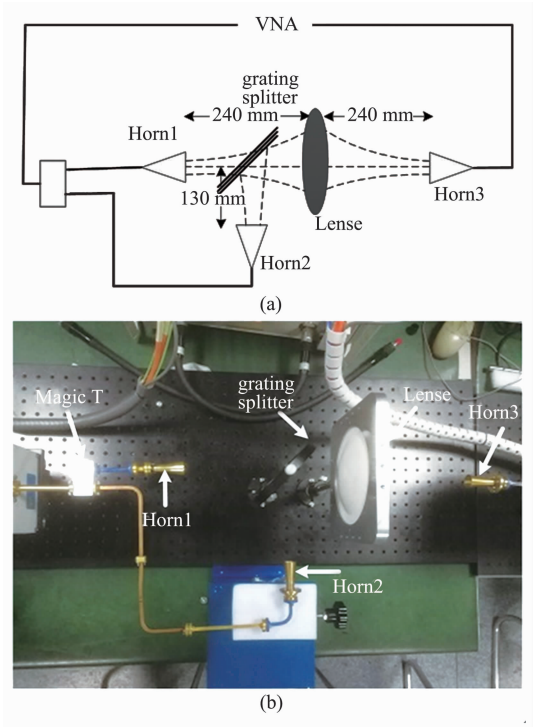

Fig. 7　Photos of (a) the schematic setup and (b) the physical test
图 7　测试系统(a)原理示意图,(b)实物图片

The test results are shown in Fig. 8. Figure 8(a) shows the S_{21} parameter for raw test data of the reflected beam, the transmitted beam and the combined and the Fig. 8(c) show the loss of long connecting waveguide and quasi-optical channel. The loss in quasi-optical channel is composed of loss of lense, loss of grating splitter and loss of some connecting waveguide, and the lens loss occupy the majority. Finally, the Fig. 8(b) is obtained from Figs. 8(a) and 8(c).

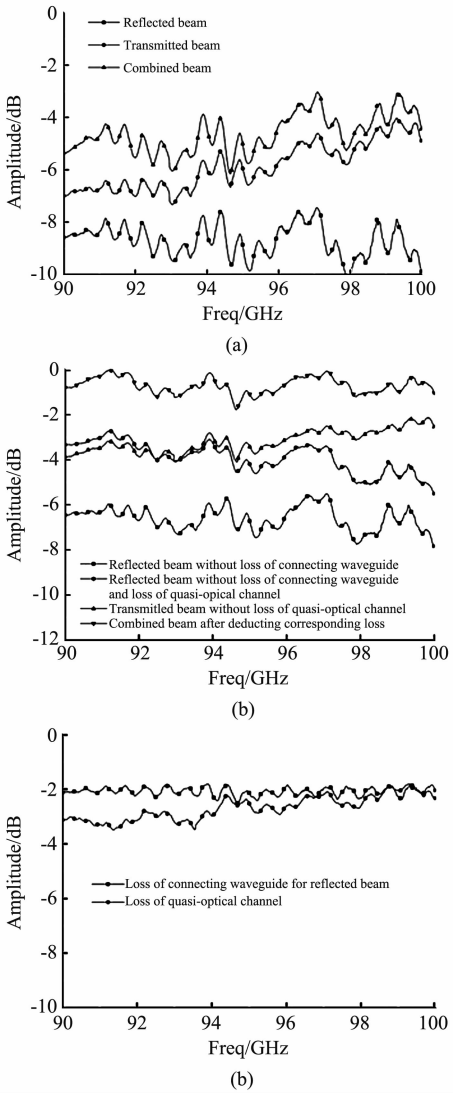

Fig. 8　Results of (a) the original data, (b) no loss, (c) loss of connecting waveguide and quasi-optical channel
图 8　结果(a)测试,(b)除去损耗,(c)连接波导和准光通道损耗

The transmission loss of the two channels is measured as shown in Fig. 8 (a). The Horn3 is twisted at a certain angle to receive the combined beam power in the quasi-optical channel from the polarization composition of the reflected beam and transmitted beam. The result for the combined beam is also shown in Fig. 8 (a). The

above test results include all kinds of loss, caused by the components and discontinuities in the channel. For example, the reflected channel includes the loss of the long connecting waveguide while the transmission channel does not include this loss, due to the spatial position. The loss of the long connecting waveguide is measured, shown as square sign in Fig. 8(c). The loss of the long waveguide connected to the reflection channel is removed, so the result is shown as square sign in Fig. 8(b) and roughly similar to the transmitted beam. In the experiment, a lens is used as the beam transformation element, while the parameters and aperture size of the existing ellipsoid mirror are not suitable for a matched Gaussian beam transformation. However, the loss in quasi-optical channel with the lense is unignorably as a result of the surface reflection and internal insertion loss of the lense, shown as round sign in Fig. 8(c). It is assumed here that the quasi-optical channel loss of the reflective branch and the transmissive branch is approximatively equal, but the transmission characteristics of the two branches are still different due to the power division characteristic of the magic-T. Then the transmission loss for the reflected beam and transmitted beam without the loss of the quasi-optical channel is shown in Fig. 8(b).

It is clear that the non-ideality of the magic-T and the difference on the loss of the reflection channel and the transmission channel makes the main polarization direction of the combined beam constantly change in the test frequency band. Based on the use of the measured transmission power of the combined channel, the reflected channel and the transmitted channel in Fig. 8(a), the angle between the combined beam polarization and the reflected beam polarization can be obtained by using the polarization relationship. Then the transmission power without the above loss can be calculated after the solved angle is brought in the calculation with the processed reflected beam and the processed transmitted beam in Fig. 8(b) and the result is shown as lower triangle sign. The loss contained in the combined beam is mainly the loss of polarization mismatch and the result shows it's less than 1 dB in the most test frequency band from 90 GHz to 100 GHz. If the amplitude of the two channels can keep constant in one frequency band, the polarization of the combined beam is also constant and then the loss of polarization mismatch may be minimal for a matching reception.

The experiment results show that it is feasible to use this scheme to achieve beam power combining. However, it maybe not suitable to be applied directly in practical applications due to the difference between the theoretical analysis and practical use. If an ellipsoid reflector is used for all the beam transformation which can minimize the transmission loss, the output beam power can be improved evidently. More research and experiment will be studied in the future.

4 Conclusions

Beam power combining approach is proposed for short millimeter wave power combining to increase the output power of source. Concept of 1 + 1 type beam power combining is presented, analyzed and simulated. Simulation results and experimental results after removing some component loss, show that a high combining efficiency over 80% can be reached at most frequency band from 90 GHz to 100 GHz. More investigation is needed for beams combining where beam parameters may be different in future. The greatest advantage of the technique is that there is low loss and no need to design complex beam transformations.

References

[1] Guillet J P, Recur B, Frederique L, *et al*. Review of terahertz tomography techniques[J]. *Journal of Infrared Millimeter & Terahertz Waves*, 2014, **35**(4), 382-411.

[2] Siemion A, Siemion A, Suszek J, *et al*. THz beam shaping based on paper diffractive optics[J]. *IEEE Transactions on Terahertz Science & Technology*, 2016, **6**(4),568-575.

[3] Tadokoro Y, Nishikawa T, Kang B, *et al*. Measurement of beam profiles by terahertz sensor card with cholesteric liquid crystals[J]. *Optics Letters*, 2015, **40**(19), 4456-4459.

[4] Chang K, Sun C. Millimeter-wave power-combining techniques[J]. *IEEE Transactions on Microwave Theory and Techniques*,1983, DOI: 10.1109/TMTT.1983.1131443.

[5] Jeon J, Kwon Y, Lee S. 1.6 and 3.3 W power-amplifier modules at 24GHz using waveguide-based power-combining structures[J]. *IEEE Transactions on Microwave Theory and Techniques*, 2000, DOI: 10.1109/22.899033.

[6] Navarro J A, Chang K. *Integrated active antennas and spatial power combining*[M]. Wiley, 1996.

[7] DeLisio M P, York R A. Quasi-optical and spatial power combining [J]. *IEEE Transactions on Microwave Theory and Techniques* 2002, **50**(3), 929-936.

[8] Saavedra C E, Wright W, Compton R C. A circuit, waveguide, and spatial power combiner for millimeter-wave amplification[J]. *IEEE Transactions on Microwave Theory and Techniques*, 1999, **47**(5), 605-613.

[9] Belaid M, Wu K. Spatial power amplifier using a passive and active TEM waveguide concept[J]. *IEEE Transactions on Microwave Theory and Techniques* , 2003, **51**(3), 684-689.

[10] Jia P, Chen L Y, Alexanian A. Broad-band high-power amplifier using spatial power-combining technique[J]. *IEEE Transactions on Microwave Theory and Techniques* , 2003, **51**(12), 2469-2475.

[11] Xie X Q, Zhao X, Liu X. A waveguide-based spatial power combining module at higher millimeter-wave frequency" [J]. *Journal of Infrared, Millimeter, and Terahertz Waves* 2013, **34**(3-4), 299-307.

[12] Keller M G, Shaker J, Antar Y M M. Millimeter-wave Talbot array illuminators[J]. *IEEE Antennas and Wireless Propagation Letters*, 2006, **5**(1), 204-208.

[13] Magath T, Hoft M, Judaschke R. *et al*. A two-dimensional quasi-optical power combining oscillator array with external injection locking. [J]. *IEEE Transactions on Microwave Theory and Techniques* , 2004, **52**(2), 567-572.

[14] Wang L, Dou W B, Meng H F. Study of millimeter wave spatial beam synthesis based on quasi-optical technology, Antennas and Propagation (APCAP) [C]. 2016 *IEEE 5th Asia-Pacific Conference on. IEEE*, 2016, 333-334.

[15] Dou W B. Application of quasi-optical techniques in THz technology [J]. Journal of microwaves (Chinese), 2013, **29**(5), 113-119.

[16] Dou W B. Millimeter wave quasi-optical theory and techniques[M]. (second edition), 2006.

[17] Goldsmith P F. *Quasioptical systems: Gaussian Beam quasioptical propagation and applications*[M]. New York: IEEE press, 1998.

[18] Wang L, Dou W B. A new type of profiled horn as an efficient gaussian beam launcher[C]. *Millimeter Wave and THz Technology Workshop (UCMMT)*,2014 7th UK,Europe,China,2014.

[19] Xu L, Wang W, Wang Y F, *et al*. Ellipsoidal reflector design for quasi-optical network[C]. *National Conference on Microwave and Millimeter Waves*. 2007.